The Photochemistry of *trans-ortho-*, *-meta-*, and *-para-*Aminostilbenes

Frederick D. Lewis,* Rajdeep S. Kalgutkar, and Jye-Shane Yang†

Contribution from the Department of Chemistry, Northwestern University, 2145 Sheridan Road, Evanston, Illinois 60208

Received July 6, 1999. Revised Manuscript Received October 15, 1999

Abstract: The photochemical behavior of the three positional isomers of *trans*-aminostilbene is reported and compared to that for unsubstituted *trans*-stilbene. The absorption spectrum of the para isomer displays a single intense long-wavelength band; however the meta and ortho isomers display two less intense bands as a consequence of configuration interaction. All three isomers are fluorescent and display similar solvent-induced shifts of their fluorescence maxima. The fluorescence rate constant of the para isomer is larger than that of the ortho or meta isomer. The para isomer has a short singlet lifetime and high photoisomerization quantum yield, similar to those for *trans*-stilbene. In contrast, the ortho and meta isomers have long singlet lifetimes and low photoisomerization quantum yields. Isomerization of the para isomer is a singlet-state process, whereas isomerization of both the ortho and meta isomers is a triplet-state process. The lower bound for the barrier for singlet-state torsion of the ortho and meta isomers is 7 kcal/mol. The barrier height is found to be determined by the effects of the amino substituent upon the relative energies of the fluorescent singlet and twisted singlet states.

Introduction

The photochemical behavior of *trans*-stilbene (**1**) and its derivatives has been the subject of intense scrutiny.[1,2] Two decay processes can account for the behavior of *trans*-stilbene in solution; fluorescence and torsion about the central double bond to yield a short-lived twisted intermediate which decays to yield an approximately equal mixture of *trans*- and *cis*-stilbene.[1] There is a small thermal barrier for the torsional process but not for fluorescence. As a consequence, the lifetime of the fluorescent singlet state is very short, and isomerization is the predominant decay process at room temperature. Intersystem crossing competes with singlet state isomerization and fluorescence in the case of some halogenated and nitro-substituted stilbenes.[3,4] Other monosubstituted stilbenes display behavior similar to that of *trans*-stilbene.[1c]

We recently reported that the photochemical behavior of several disubstituted aminostilbenes is highly dependent upon the position of the amine substituent.[5] Substituted *trans*-4-aminostilbenes display behavior similar to that of stilbene (short singlet lifetime and large isomerization quantum yields), whereas *trans*-3-aminostilbenes display long singlet lifetimes and large fluorescence quantum yields. The behavior of meta- and para-substituted stilbenes is in most cases similar; however, a few exceptions to this generalization have been reported.[6,7] Moreover, meta-substituted benzenoid compounds are observed to be more reactive than their para isomers toward photochemical solvolysis reactions, a phenomenon known as the "meta effect".[8] Recent studies by Zimmerman using CASSCF calculations led to the suggestion that ortho substituents should display enhanced reactivity similar to the meta isomers, the "meta−ortho" effect.[8] Whereas a small number of studies have compared the photochemical behavior of meta- and para-substituted stilbenes, ortho-substituted stilbenes have been largely ignored.

We report here the results of an investigation of the photochemical behavior of the trans isomers of *ortho*- (**2**), *meta*- (**3**), and *para*-aminostilbene (**4**). As previously observed for several donor−acceptor disubstituted aminostilbenes, the meta isomer is found to have a substantially longer singlet lifetime than the para isomer.[5] In addition, the behavior of the ortho isomer is found to be similar to that of the meta isomer. The origin of this pronounced effect of positional isomerization on photochemical reactivity is elucidated.

Results and Discussion

Electronic Absorption Spectra. The absorption spectra of aminostilbenes **2**−**4** in hexane solution are shown in Figure 1. The spectrum of **4** resembles that of *trans*-stilbene (**1**), consisting of a single intense long wavelength band.[9] The absorption maximum of **4**[10,11] is intermediate in energy between that of **1** and 4-dimethylaminostilbene[12] as expected on the basis of the

* To whom correspondence should be addressed. E-mail: lewis@chem.nwu.edu.

† Present address: Department of Chemistry, National Central University, Taiwan, R. O. C.

(1) (a) Saltiel, J.; Sun, Y.-P. *Photochromism, Molecules and Systems*; Durr, H., Boaus-Laurent; H., Eds.; Elsevier: Amsterdam, 1990; p 64 and references therein. (b) Waldeck, D. H. *Chem. Rev.* **1991**, *91*, 415. (c) Saltiel, J.; Charlton, J. L. *Rearrangements in Ground and Excited States*; de Mayo, P., ed.; Academic Press: New York, 1980; Vol. 3, p 25.

(2) Recent representative publications in the area of donor−acceptor stilbenes are: (a) Abraham, E.; Oberle, J.; Jonusauskas, G.; Lapouyade, R.; Rulliere, C. *J. Photochem. Photobiol., A* **1997**, *105*, 101. (b) Il'ichev, Y. V.; Kühnle, W.; Zachariasse, K. A. *Chem. Phys.* **1996**, *211*, 441. (c) LeBreton, H.; Bennetau, B.; Letard, J. F.; Lapouyade, R.; Rettig, W. *J. Photochem. Photobiol., A* **1996**, *95*, 7. (d) Görner, H. *Ber. Bunsen Phys. Chem.* **1998**, *102*, 726. (e) Rettig, W. *Top. Curr. Chem.* **1994**, *169*, 253.

(3) Saltiel, J.; Marinari, A.; Chang, D. W.-L.; Mitchener, J. C.; Megarity, E. D. *J. Am. Chem. Soc.* **1979**, *101*, 2982.

(4) Görner, H.; Schulte-Frohlinde, D. *J. Phys. Chem.* **1979**, *83*, 3107.

(5) Lewis, F. D.; Yang, J.-S. *J. Am. Chem. Soc.* **1997**, *119*, 3834.

(6) Güsten, H.; Klasinc, L. *Tetrahedron Lett.* **1968**, *26*, 3097.

(7) Lapouyade, R.; Kuhn, A.; Letard, J.-F.; Rettig, W. *Chem. Phys. Lett.* **1993**, *208*, 48.

(8) Zimmerman, H. E. *J. Phys. Chem. A.* **1998**, *102*, 5616 and references therein.

(9) Gegiou, D.; Muzkat, K. A.; Fischer, E. *J. Am. Chem. Soc.* **1968**, *90*, 3907.

10.1021/ja992335q CCC: $18.00
Published on Web 12/08/1999

Table 1. Observed and Calculated Spectroscopic Parameters

		absorption max (λ_{max}/nm)[a]	molar absorptivity (log ϵ_{max})	fl. max (λ_{max}/nm)	0,0 (λ/nm)	Stokes shift/ cm^{-1} [b]	oscillator strength (f)[c]
1	hexane	294, (307, 321)[d]	4.45[d]	347[e]	326[e]	2545	0.75[f]
	acetonitrile	294, (308, 320)	4.47, (4.46, 4.26)	347	325	2663	0.76
2	hexane	286, 334	4.25, 4.11	407	373	2319	0.23
	acetonitrile	291, 346	4.25, 4.08	445	398	2993	0.23
3	hexane	298, (311, 329)	4.38, (4.28, 3.94)	387	356	2719	0.12
	acetonitrile	300, (312, 332)	4.41, (4.30, 3.90)	446	384	3906	0.12
4	hexane	316, (332)	4.50, (4.47)	380	354	2367	0.86
	acetonitrile	(318), 336	(4.49), 4.51	423	378	3127	0.92

[a] Shoulders in parentheses. [b] Calculated by Berlman's method.[17a] [c] $f = 4.3 \times 10^{-9} \int(\bar{\nu})d\bar{\nu}$. [d] From ref 15, in heptane. [e] From ref 36, in methylpentanes. [f] From ref 11a.

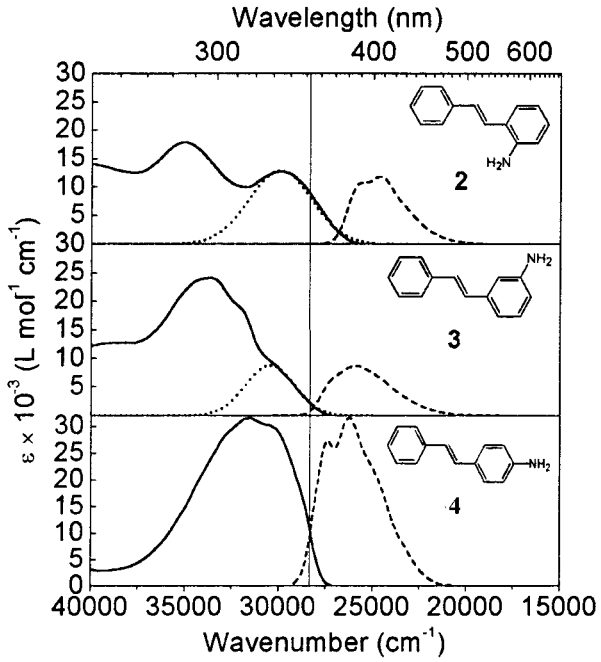

Figure 1. Molar absorptivity (solid lines) and emission (arbitrary intensity, long dashed lines) spectra of **2**−**4** in hexane solution. Gaussian deconvolutions of the longest wavlength transition in the absorption spectra of **2** and **3** are shown as dotted lines.

donor strength of the substituent. The spectra of **2** and **3** are more complex than that of **1** or **4**. Two long wavelength maxima are observed for **2,** whereas a maximum with shoulders are observed for **3**.[10] More complex spectra might arise from the presence of two ground-state rotamers; however, both experimental and computational results (vide infra) indicate that both rotamers of **2** and **3** should have the same spectra. The absorption spectra of **3**−**4** show only modest solvent induced shifts in acetonitrile vs hexane solution (≤4 nm), whereas a slightly larger solvent shift (12 nm) is observed for **2** in acetonitrile (Table 1).

The appearance of the absorption spectra of **2**−**4** are similar to those of some disubstituted benzene derivatives possessing two mesomeric substituents.[13] Whereas para-disubstituted benzene derivatives display only a single long wavelength band, ortho- and meta-disubstituted derivatives generally possess two long wavelength bands, with the band splitting being greater for ortho than for meta compounds.[14] Molecular orbital calculations[13] suggest that the origin of this behavior in disubstituted benzene derivatives may be due to symmetry-induced configuration interaction in the ortho and meta cases but not in the para case. In the case of para-disubstituted benzene derivatives (C_{2v}), transitions of unlike symmetry (A and B) do not show configuration interaction as they belong to different irreducible representations. In the case of the ortho- and meta-disubstituted benzene derivatives (C_s), the reduction of symmetry results in extensive configuration interaction between pure transitions and a resultant splitting of the state energy levels that is slightly larger for ortho vs meta compounds. The absorption spectra of **2** and **3** (Figure 1) are similar to those of disubstituted benzenes. Hence, **2** and **3** may be thought of as substituted anilines that possess lowered symmetry. It should be pointed out that the splitting of absorption bands occurs only in the case of mesomeric substituents and not in the case of alkyl substituents. Sterically hindered stilbenes such as 2,4,6-trimethylstilbene and 2,2′,4,4′,6,6′-hexamethylstilbene display a single long wavelength band that has reduced intensity and vibronic structure and is blue-shifted compared to stilbene, as expected from theoretical considerations of orbital energies.[9] A similar loss of intensity along with a blue shift of the long wavelength band has been observed for 4-(dimethylamino)-2′,6′-dimethylstilbene.[11]

The oscillator strengths of the long wavelength absorption band have been estimated for **2**−**4** in hexane and acetonitrile solvents (Table 1). Integration of the molar absorptivity curve is straightforward for **4**, since the long wavelength band is well-resolved from other, higher energy bands. In the case of **2** and **3**, the lowest-energy transitions overlap partially with more intense, higher-energy transitions and therefore their lowest-energy transitions are approximated as Gaussian curves (Figure 1). The basic assumption in this approach is that each spectral band represents an excitation to a single state.[15] Integration of the deconvoluted Gaussian bands for **2** and **3** provided the integral area required to compute the oscillator strength.[16] The calculated oscillator strengths are given in Table 1. Values for **2** and **3** are smaller than those for **1** and **4** in both hexane and acetonitrile solution.

Fluorescence Spectra. The fluorescence spectra of **2**-**4** in hexane are also shown in Figure 1. They display varying degrees of vibronic structure in nonpolar solvents. The fluorescence spectra of **1** and **4** are similar in appearance and the fluorescence maximum of **4** is intermediate between those of **1** and

(10) Jungmann, H.; Güsten, H.; Schulte-Frohlinde, D. *Chem. Ber.* **1968**, *101*, 2690.

(11) (a) Beale, R. N.; Roe, E. M. F. *J. Am. Chem. Soc.* **1952**, *74*, 2302. (b) Haddow, A.; Harris, R. J. C.; Kon, G. A. R.; Roe, E. M. F. *Philos. Trans. R. Soc.* **1948**, *241*, 147.

(12) Létard, J.-F.; Lapouyade, R.; Rettig, W. *J. Am. Chem. Soc.* **1993**, *115*, 2441.

(13) Murrell, J. N. *The Theory of the Electronic Spectra of Organic Molecules*; John Wiley And Sons: New York, 1963.

(14) (a) Grinter, R.; Heilbronner, E.; Godfrey, M.; Murrell, J. N. *Tetrahedron Lett.* **1961**, *21* 771. (b) Grinter, R.; Heilbronner, E. *Helv. Chem. Acta* **1962**, *45*, 2496.

(15) Jaffe, H. H.; Orchin, M. *Theory and Applications of Ultraviolet Spectrocopy*; John Wiley and Sons: New York, 1962.

(16) Klessinger, M.; Michl, J. *Excited States And Photochemistry Of Organic Molecules*; VCH Publishers: New York, 1995.

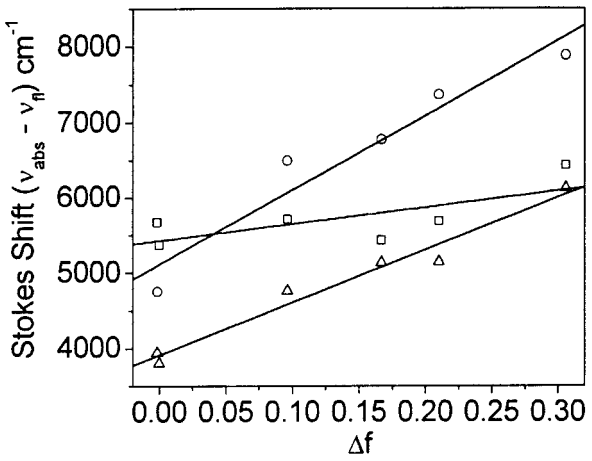

Figure 2. Lippert−Mataga plot for **2** (□), **3** (○), and **4** (△). The Δf parameter is calculated according to eq 1 for hexane, cyclohexane, dibutyl ether, diethyl ether, tetrahydrofuran, and acetonitrile in order of increasing polarity.

4-dimethylaminostilbene.[12] The $S_0 \rightarrow S_1$ transition energies for **3** and **4** in hexane are similar, indicating that both isomers show similar stabilization of the relaxed Franck−Condon state (Figure 1) whereas the $S_0 \rightarrow S_1$ transition for **2** in hexane is red-shifted by about 4 kcal/mol relative to the $S_0 \rightarrow S_1$ transition for **3** or **4**. The red-shifted $S_0 \rightarrow S_1$ transition for **2** may result from the larger splitting of the absorption band due to configuration interaction (vide infra).[14b] The Stokes shifts for **1**−**4** can be calculated according to Berlman's method as the difference between the 0,0 transition and the center of gravity of the fluorescence spectrum.[17a] The Stokes shift for **2**−**4** in hexane is 2500 ± 200 cm^{-1} and slightly larger in acetonitrile (3450 ± 450 cm^{-1}) suggesting that there is no "extra" stabilization of the emissive state via large amplitude nuclear motion (Table 1).

The spectra of **2**−**4** in medium polar-to-polar solvents are broad and lack vibronic structure. Upon increasing the polarity of the medium, the fluorescence spectra shift to longer wavelengths (Table 1 and Figure 2). The solvent-polarity-induced shift can be used to determine the dipole moment of the excited state using the Lippert−Mataga equation (equation 1).[18]

$$\bar{\nu}_{abs} - \bar{\nu}_{fluo} = \frac{2\mu_e(\mu_e - \mu_g)}{hca^3} \cdot \Delta f, \quad \text{where} \quad \Delta f = \left[\frac{\epsilon - 1}{2\epsilon + 1} - \frac{\eta^2 - 1}{2\eta^2 + 1}\right] \quad (1)$$

where ν_{abs} and ν_{fluo} are the absorption and fluorescence maxima, μ_g and μ_e are the ground and excited-state dipole moments, a is the solvent cavity radius in Å, ϵ is the solvent dielectric, and η is the solvent refractive index. The ground-state dipole moments of **2**−**4** have previously been determined from their measured dielectric constants and refractive indices (Table 2).[19] The excited-state dipole moments of **2**−**4**, calculated from eq 1 are given in Table 2, and their values increase in the order **2** < **4** < **3**. The smaller excited-state dipole moment of **2** may be attributed to the large solvatochromic shift in its absorption spectra, possibly due to specific solvation of its nonplanar structure, thereby reducing the observed Stokes shift and ultimately its excited-state dipole moment. The excited-state dipole moments of **2**−**4** are smaller than that of 4-(dimethylamino)-4′-cyanostilbene (21 D), consistent with the absence of strong acceptor in **2**−**4**.[2b] Although excited-state dipole moments are not expected to be a sum of component bond moments as they are in the ground state, the observed decrease in the ortho position is expected based on earlier work by Sinha and Yates.[20]

Table 2. Ground and Excited-State Dipole Moments for **2**−**4**

	solvatochromic slope/cm^{-1} [a]	μ_g/D[b]	μ_e/D[c,d]
2	2208	1.5	6.0
3	9881	1.5	11.9
4	6641	2.1	10.2

[a] Calculated based on eq 1. [b] From ref 19. [c] Assuming solvent cavity, a = 5 Å. [d] 95% confidence interval is ± 1.0 D.

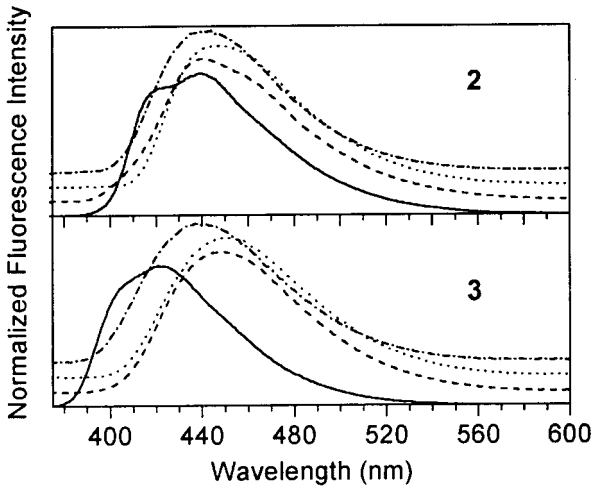

Figure 3. Temperature dependence of the fluorescence spectra of **2** and **3** in MTHF. The spectra are at the following temperatures: — 80 K; - - - - 120 K; ··· 200 K; -·-·-· 280 K. Baseline offset increases with increasing temperature.

The temperature dependence of the fluorescence spectra of **2** and **3** has been studied in 2-methyltetrahydrofuran (MTHF) between 280 and 80 K. The fluorescence spectra of **2** and **3** show no change in shape as the temperature is lowered, although there is a slight red shift (6 and 12 nm, respectively) upon cooling from 280 to 200 K (Figure 3). On further cooling a blue shift is observed, and below 120 K the fluorescence spectra of **2** and **3** are blue-shifted relative to the room-temperature spectra. The emission spectra of both **2** and **3** at 80 K resemble their room-temperature spectra in nonpolar solvents (Figure 3). This behavior is consistent with the temperature dependence of the dielectric constant of MTHF which is reported to increase with decreasing temperature followed by a sudden drop near the glass transition temperature of the solvent (approximately 120 K).[21] Due to the absence of any large spectral shifts on lowering the temperature, it can be concluded that there are no large amplitude excited-state geometry changes for **2** and **3**.

The quantum yields for fluorescence, ϕ_f, of **2**, **3**, and **4** have been measured in cyclohexane and acetonitrile solution and the results are reported in Table 3. The ϕ_f values for **2**−**4** decrease

(17) (a) Berlman, I. B. *Handbook of Fluorescent Spectra of Aromatic Molecules*, 2nd ed.; Academic Press: New York, 1971; pp 27−28. (b) Berlman, I. B. *Handbook of Fluorescent Spectra of Aromatic Molecules*, 2nd ed.; Academic Press: New York, 1971; pp 74−75.

(18) (a) Lippert, E. *Z. Elektrochem.* **1957**, *61*, 962. (b) Mataga, N.; Kaifu, Y.; Koizumi, M. *Bull. Chem. Soc. Jpn.* **1956**, *29*, 465. (c) Liptay, W. Z. *Z. Naturforsch.* **1965**, *20a*, 1441.

(19) Everard, K. B.; Kumar, L.; Sutton, L. E. *J. Chem. Soc.* **1951**, 2807, 2812.

(20) Sinha, H.; Yates, K. *J. Am. Chem. Soc.* **1991**, *113*, 6062.

(21) Furutsuka, T.; Imura, T.; Kojima, T.; Kawabe, K. *Technol. Rep. Osaka Univ.* **1974**, 367.

Table 3. Quantum Yields of Fluorescence (ϕ_f), Photoisomerization (ϕ_i), Singlet Lifetimes (τ_s), and Rate Constants of Fluorescence (k_f)

		ϕ_f	ϕ_i [a]	τ_s/ns	k_f (expt)/s^{-1}	k_f (calc)/s^{-1} [b]	k_f^0 (fit)/s^{-1} [h]	k_f^0 (rt)/s^{-1} [i]
1	hexane	0.04[c]	0.52[d]	0.070[e]	6.0×10^8 [c]	5.9×10^8 [c]	3.8×10^8 [c]	
2	cyclohexane	0.88	0.04	3.7	2.4×10^8	1.4×10^8 [g]	1.3×10^8 [h,j]	1.3×10^8 [j]
	acetonitrile	0.69	0.12	5.4	1.3×10^8	1.1×10^8		
3	cyclohexane	0.78	0.09	7.5	1.0×10^8	0.8×10^8 [g]	5.8×10^7 [h,j]	6.0×10^7 [j]
	acetonitrile	0.40	0.23	11.7	0.3×10^8	0.5×10^8		
4	cyclohexane	0.05	0.49[f]	~0.1	~5.0×10^8	5.9×10^8 [g]		
	acetonitrile	0.03	0.52	~0.1	~3.0×10^8	4.6×10^8		

[a] Excitation at 313 nm. [b] Calculated by eq 2. [c] From ref 22. [d] In pentane, from ref 1b. [e] From ref 26. [f] From ref 6. [g] In hexane solution. [h] Calculated by fitting temperature dependent τ_s to eq 4 without the activation term. [i] Calculated from room-temperature data: $\phi_f \tau_s^{-1}/\eta^2$; $\eta = 1.35141$ at 25 °C (ref 30). [j] In isopentane.

on going from nonpolar to polar solvents. Values of ϕ_f for **4** are similar to those determined for *trans*-stilbene;[1,22] however, values of ϕ_f for **2** and **3** are substantially higher. Such high quantum yields are unusual for nonrigid stilbenes, but have been reported for 4,4′-dimethoxystilbene in hexane ($\phi_f = 0.91$[23]) and 4,4′-diaminostilbene in dioxane ($\phi_f = 0.76$[24]).

Singlet lifetimes, τ_s, have been measured for **2**−**4** in cyclohexane and acetonitrile solutions and the results are given in Table 3. The lifetime of **4** is similar to that of **1** (0.108 ns in 3:2 methylcyclohexane/isohexane,[25] 0.070 ns in hexane at 296.2 K[26]), and both molecules have similar fluorescence quantum yields.[1] Thus, the fluorescence rate constants ($k_f = \phi_f \cdot \tau_s^{-1}$) for both compounds are similar. The singlet lifetimes of **2** and **3** are unusually long when compared to those for **4** and **1**. Single-exponential decay is observed for **2** and **3**, even though both are expected to exist as a mixture of rotamers. Either one rotamer predominates, or both rotamers have the same decay time. It is also possible that one rotamer is nonfluorescent; however, in view of the large fluorescence quantum yields in nonpolar solvent (Table 3) it would have to be the minor rotamer. Increasing solvent polarity causes a decrease in k_f for **2**−**4**, resulting in a increase in τ_f and decrease in ϕ_f (Table 3).

The rate constant of fluorescence can be calculated using the Strickler−Berg relationship (equation 2)[27]

$$k_f = 2.889 \times 10^{-9}\, \eta^2 \frac{\int_0^\infty f(\bar{\nu})\mathrm{d}\bar{\nu}}{\int_0^\infty f(\bar{\nu})\bar{\nu}^{-3}\,\mathrm{d}\bar{\nu}} \int_0^\infty \frac{\epsilon(\bar{\nu})\mathrm{d}\bar{\nu}}{\bar{\nu}} \qquad (2)$$

where $f(\bar{\nu})$ and $\epsilon(\bar{\nu})$ are the fluorescence intensity and molar absorptivity obtained from the fluorescence and absorption spectra, respectively, and η is the refractive index of the solvent. The calculated values of k_f agree quite well with those obtained experimentally based on the fluorescence quantum yields and singlet lifetime data (Table 3). The calculated k_f's for **2** and **3** are lower than those for **4**, in accord with lower oscillator strength for the $S_0 \rightarrow S_1$ transition in **2** and **3**. The calculated k_f value for **4** in hexane is similar to that of **1**.[1a] The decreased value of k_f in polar solvents may result, at least in part from the a shift in the $\langle \tilde{\nu}^{-3} \rangle_{av}^{-1}$ term in the Strickler−Berg equation to lower energy, although the Franck−Condon factors may also be important.

The singlet lifetime of **4** in isopentane solution increases from ~0.1 ns at room temperature to 1.2 ns at 77 K. A similar increase has been observed for **1**.[25] The singlet lifetimes of **2** and **3** have been determined in isopentane from 77 K to ambient temperature and the data obtained is presented in Table 4. Single-exponential decay is observed at all temperatures. It is of interest to note that unlike the behavior of *trans*-stilbene[25] or **4**, the lifetimes of **2** and **3** do not decrease between 160 and 300 K, and in fact a slight increase due to changes in solvent refractive index is noted.[22,28] Below 160 K, there is an sudden decrease in the lifetime for **3**, and thereafter the lifetime remains constant on further cooling, whereas in the case of **2** there is a continuous decrease in the fluorescent lifetime (Table 4). Changes in the fluorescent lifetime upon cooling below 160 K may be interpreted as arising from either loss of a nuclear relaxation pathway[12] or from loss of orientational polarization of an excited-state dipole by slowing down solvent reorganization.[2b] However, the data above 160 K for **2** and **3** clearly indicates that no activated decay process such as twisting about the double bond competes with fluorescence.

Table 4. Temperature Dependence of τ_s for **1**−**4** in Isopentane

	τ_s/ns			
T (K)	**1**	**2**	**3**	**4**
77	1.65[a]			1.2
80		2.4	6.0	
100		2.3	5.9	
120		2.3	6.2	
140		3.0	6.2	
160		3.2	7.3	
180		3.6	7.3	
200		3.5	7.3	
220		3.6	7.3	
240		3.8	7.4	
260		3.7	7.4	
280		3.8	7.4	
298	0.070[b]	3.7	7.5	~ 0.1

[a] In 3:2 methylcyclohexane/isopentane. From ref 25. [b] From ref 26.

Electronic Structure. The electronic structure and spectra of the aminostilbenes have been further investigated by means of semiempirical INDO/S-SCF-CI (ZINDO) calculations using the algorithm developed by Zerner and co-workers.[29] Ground-state molecular structures were obtained from AM1 calculations. The calculated ground-state geometry of **3** is quasi-planar (aniline−styrene torsion angle is 26° for **3** and 0° for **4**), whereas the ground state of **2** has a styryl−aniline dihedral angle of 42−48°. The ZINDO-derived frontier molecular orbitals for **3** are shown in Figure 4. Corresponding orbitals for **2** and **4** are provided in the Supporting Information. The HOMO and LUMO orbitals of **2**−**4** resemble those of **1**, aside from the presence of the nitrogen p orbital which has a larger orbital coefficient in

(22) Saltiel J.; Waller, A. S.; Sears, D. F., Jr.; Garrett, C. Z. *J. Phys. Chem.* **1993**, *97*, 2516.
(23) Zeglinski, D. M.; Waldeck, D. H. *J. Phys. Chem.* **1988**, *92*, 692.
(24) Smit, K. J.; Ghiggino, K. P. *Chem. Phys. Lett.* **1985**, *122*, 369.
(25) Sumitani, M.; Nakashima, N.; Yoshihara, K.; Nagakura, S. *Chem. Phys. Lett.* **1977**, *51*, 183.
(26) Kim, S. K.; Courtney, S. H.; Fleming, G. R. *Chem. Phys. Lett.* **1989**, *159*, 543 and references therein.
(27) (a) Strickler, S. J.; Berg, R. A. *J. Chem. Phys.* **1962**, *37*, 814. (b) Birks, J. B.; Dyson, D. J. *Proc. R. Soc. London, Ser. A* **1963**, *275*, 135.
(28) Rückert, I.; Demeter, A.; Morawski, O.; Kühnle, W.; Tauer, E.; Zachariasse, K. A. *J. Phys. Chem. A* **1999**, *103*, 1958.
(29) Zerner, M. C.; Loew, G. H.; Kirchner, R. F.; Mueller-Westerhoff, U. T. *J. Am. Chem. Soc.* **1980**, *102*, 589.

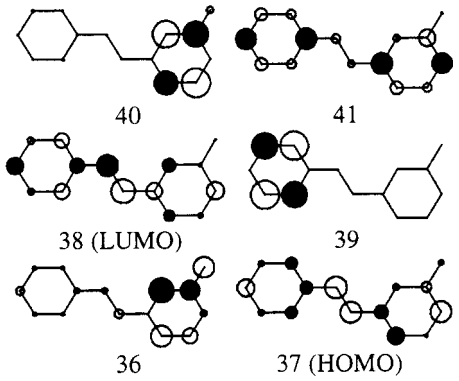

Figure 4. Frontier molecular orbitals for **3** as optimized by ZINDO.

the HOMO than the LUMO. To the extent that the HOMO → LUMO transition contributes to the lowest-energy transition, the lowest excited singlet states should possess aniline → styrene charge-transfer character, in accord with the observation of solvatochromic shifts for their fluorescence spectra.

The calculated energies of the ground and first two excited singlet states of **1**−**4** are reported in Table 5 along with the calculated oscillator strengths and configuration interaction descriptions of the excited states. In the case of **2** and **3** data is reported for both of the ground-state rotamers. The energy difference, as calculated by AM1, between the lower-energy (see Figure 1 for structures) and higher-energy rotamers is only 0.11 and 0.15 kcal/mol, respectively. Their calculated S_1 and S_2 energies are identical. The calculated ground-state energies for **2**−**4** are similar despite the nonplanarity of **2**. The lowest-energy transition for **4**, like that of **1**, is an allowed, essentially pure HOMO to LUMO π,π^* transition. The calculated and observed singlet energies for **4** (Tables 1 and 5) are in good agreement: however, the calculated oscillator strengths are higher than the values obtained from the integrated absorption spectra (Table 1). The second singlet states for both **4** and **1** are predicted to have extensive configuration interaction and low oscillator strengths. Both of the two lowest singlet states calculated for **2** and **3** have extensive configuration interaction and more equal oscillator strengths, as previously reported for other ortho- and meta-disubstituted benzene derivatives with mesomeric substituents.[14,16] The contribution of the HOMO → LUMO configuration to the description of ^{1}S* is substantially smaller for **2** and **3** (∼50%) than for **4** or **1** (> 95%). The ZINDO calculations are consistent with the observation of two low-energy transitions for **2** and **3** (Figure 1). The calculated and observed S_2 energies are in reasonable agreement; however, the calculated ^{1}S* energies and oscillator strengths are higher than the observed values, particularly in the case of **2**. Splitting of the lowest energy π,π^* transition of 4-(dimethylamino)-3′-nitrostilbene has previously been reported Lapouyade et al.[7] based on CNDO/S calculations. In this case, the calculated oscillator strength for the lower-energy transition is significantly lower than for the higher-energy transition and no maximum or shoulder is apparent in the absorption spectrum.

Several important conclusions concerning the fluorescent singlet states of **2**−**4** can be drawn from the spectral data and electronic structure calculations.

(a) On the basis of the fluorescence solvatochromic shifts and calculations, the singlet states of **2**−**4** are shown to possess similar dipole moments and degrees of aniline → styrene charge-transfer character.

(b) On the basis of the absence of large Stokes shifts or strongly temperature-dependent fluorescence, the geometry of the fluorescent singlet states are shown to be similar to those of the ground state.

(c) As a consequence of more extensive configuration interaction in **2** and **3** vs **4**, the singlet oscillator strengths and fluorescence rate constants are lower for **2** and **3** than for **4**.

(d) On the basis of the observation of temperature-dependent lifetimes for **4**, but not for **2** or **3**, a thermally activated decay process is shown to compete with fluorescence in the case of **4** but not **2** or **3**.

Photoisomerization. Quantum yields for photoisomerization (ϕ_i) of **2**−**4** in cyclohexane solution are reported in Table 3. As previously observed by Güsten and Klasinc[6] the value of ϕ_i for **4** in cyclohexane is similar to that of stilbene. Significantly smaller quantum yields are observed for **2** and **3**. In fact, the values of ϕ_i for **2** and **3** are, to our knowledge, the lowest that have been observed for a monosubstituted stilbene derivative.[1c] The efficiency of photoisomerization increases substantially with increasing solvent polarity for **2** and **3**, but only slightly for **4**.

Both singlet- and triplet-state mechanisms have been thoroughly characterized for the photoisomerization of *trans*-stilbene and its derivatives.[1,3,4] Stilbene serves as the prototype for the singlet-state mechanism. A small barrier (E_{act} = 3.5 kcal/mol, $A = 10^{12.6}$) for torsion about the central double bond separates the planar fluorescent ^{1}S* state from the perpendicular ^{1}P* state which decays with similar probability to the trans and cis ground states.[1] Thermally activated barrier crossing competes effectively with fluorescence at room temperature, but less so at lower temperatures, resulting in a temperature-dependent singlet lifetime (Table 4).[25] The stilbene triplet can be populated by triplet sensitization and undergoes barrierless twisting to the perpendicular triplet.[1] Intersystem crossing from ^{1}S* is estimated to occur with a rate constant $k_{isc} = 3.9 \times 10^7$ s^{-1} but does not compete with fluorescence ($k_f = 6.0 \times 10^8$ s^{-1}) and torsion on the singlet state surface at room temperature ($k \approx 10^{10}$ s^{-1} at ambient temperature).[1a] However, significant intersystem crossing is observed for singlet stilbenes with halogen or nitro substituents.[3,4] Intersystem crossing rates for these molecules are substantially larger than for stilbene. For example, in the case of 3-bromostilbene $k_{isc} = 4.0 \times 10^9$ s^{-1} resulting in intersystem crossing being a major decay pathway for its excited singlet state.[4]

The singlet lifetime of **4** increases from 0.1 ns at room temperature to 1.2 ns at 77 K, similar to the increase reported for **1** upon cooling.[25] The room-temperature quantum yields for photoisomerization and fluorescence of **4** and **1** are also similar (Table 3). Thus, it is reasonable to assume that **4** isomerizes via a singlet-state mechanism. The barrier for singlet-state torsion in **4** can be estimated from the singlet lifetime and photoisomerization quantum yield using eq 3, assuming the value of $A_0 = 10^{12.6}$ reported for stilbene. The calculated singlet barrier for **4** is 3.5 kcal/mol, similar to that reported for **1**.

$$E_{act} = -RT \ln\left(\frac{2\phi_i \tau^{-1}}{A_0}\right) \qquad (3)$$

In contrast to the temperature-dependent lifetimes of **4** and **1**, the singlet lifetimes of **2** and **3** are independent of temperature between 298 and 160 K (Table 4). This suggests that no activated process for decay of the fluorescent ^{1}S* state competes with the nonactivated processes, fluorescence and intersystem crossing, at room temperature or below. Thus, photoisomerization of **2** and **3** is concluded to occur via intersystem crossing followed by barrierless torsion on the triplet surface. Assuming that the twisted triplet decays to yield a 1:1 ratio of trans and

Table 5. Results of the INDO/S-CIS-SCF (ZINDO) Calculations for the Lowest Singlet States of **1**−**4**

	S_0[a]	S_1			S_2		
	ΔH_f kcal/mol	ΔE/nm	f[c]	description[b]	ΔE/nm	f[c]	description[b]
1	60.89	301	1.265	34:35 (0.97)	286	0.015	31:37 (0.12), 32:35 (0.13), 32:38 (0.12), 33:35 (0.13), 34:36 (0.21), 34:37 (0.25)
2	59.70 (59.81)[d]	306 (306)[d]	0.493 (0.397)[d]	36:41 (0.10), 37:38 (0.56), 37:40 (0.16)	286 (285)[d]	0.322 (0.114)[d]	36:38 (0.12), 37:38 (0.26), 37:39 (0.12), 37:40 (0.17)
3	59.51 (59.66)[d]	308 (308)[d]	0.577 (0.588)[d]	36:38 (0.12), 37:38 (0.51), 37:40 (0.20)	296 (297)[d]	0.693 (0.656)[d]	36:38 (0.30), 37:38 (0.44), 37:40 (0.13)
4	59.11	316	1.328	37:38 (0.95)	302	0.065	34:39 (0.16), 37:39 (0.62)

[a] Geometry optimized using the AM1 Hamiltonian as implemented by the MOPAC package under Cache, Release 3.5 (Cache Scientific). [b] Orbital numbers of the pure configurations are given and the weight of each configuration is given in parentheses. Only configurations with 10% or greater contribution are included. The HOMO for **1** is orbital 34 and for **2**−**4** is orbital 37. [c] Oscillator strength. [d] Values in parentheses are for the conformer obtained by rotating the molecules shown in Figure 1 by 180° about the aniline−styrene bond. See Supporting Information for a complete table.

cis isomers, quantum yields and rate constants for intersystem crossing can be estimated from the measured isomerization quantum yields and lifetimes ($\phi_{isc} = 2\phi_i$, $k_{isc} = \phi_{isc}\tau_s^{-1}$). The sum of the quantum yields for fluorescence and intersystem crossing for both **2** and **3** in hexane solution are within the experimental error of 1.0, in accord with the absence of singlet-state isomerization or nonradiative decay. The calculated values of k_{isc} for **2** and **3** are 2.2 and 2.4×10^7 s^{-1}, respectively, similar to the value for **1** ($3.9 \times 10^7 \pm 2.3 \times 10^7$ s^{-1}) estimated by Saltiel.[1] Thus, the occurrence of triplet isomerization for **2** and **3** is a consequence of their abnormally long singlet lifetimes, rather than rapid intersystem crossing such as that observed for halostilbenes.[4]

Increasing solvent polarity results in an increase in both the singlet lifetime and isomerization quantum yield. Assuming that isomerization remains a triplet-state process in acetonitrile, the calculated values of $k_{isc} = 4.4$ and 3.9×10^7 s^{-1} for **2** and **3**, respectively. These values are approximately twice as large as those obtained in cyclohexane solution, plausibly reflecting smaller singlet−triplet splitting in the more polar solvent.

A lower bound for the barrier to torsion on the singlet surface can be estimated by modeling the temperature dependence of the singlet lifetimes, τ_s, using eq 4, assuming that both the gas-phase radiative rate constant, k_f^0, and k_{isc} are independent of temperature, the refractive index, η, is temperature-dependent,[30] and that the pre-exponential for singlet torsion $A_0 = 10^{12}$ s^{-1}.

$$\tau_s = \frac{1}{k_f^0 \cdot \eta^2 + k_{isc} + A_0 \exp\left(\frac{-E_{act}}{RT}\right)} \qquad (4)$$

The values for k_f^0 for **2** and **3** obtained by fitting the temperature-dependent fluorescence lifetimes to eq 4 but without the activated nonradiative term are similar to those obtained from the fluorescence quantum yield data and singlet lifetimes at ambient temperature ($\phi_f \cdot \tau_s^{-1}/\eta^2$)(Table 3). Improved fits are obtained by allowing the refractive index exponent to assume nonintegral values (see Supporting Information) although the residuals from the η^2 fits are within experimental error.[31] The k_f^0 term so obtained was then used in eq 4 to estimate the minimum activation barrier to singlet isomerization. Literature values of A_0 for alkene isomerization lie in the range $10^{12} - 10^{13}$ s^{-1}.[1b,c,4] Assumption of a value at the lower end of this range provides the lowest activation energy, E_{act}. The results of kinetic modeling (see Supporting Information) of the singlet lifetime vs temperature for several trial values of E_{act} is shown in Figure 5 along with experimental lifetimes. Inspection of Figure 5 provides values of $E_{act} \geq 7$ kcal/mol for both **2** and **3**. To our knowledge, these barriers are the largest observed for a monosubstituted, unconstrained stilbene derivative.

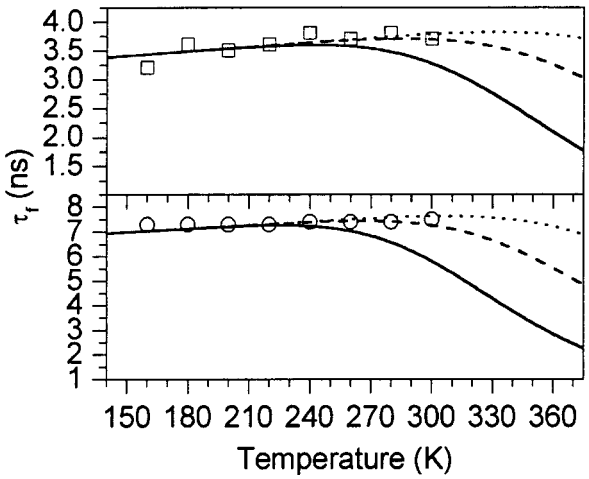

Figure 5. Temperature dependence of fluorescence lifetime for **2** (□) and **3** (○) in isopentane between 160 and 300 K. The fitted lines are based on eq 4 and are as follows: k_{isc} (**2**) $= 2.2 \times 10^7$ s^{-1} and k_{isc} (**3**) $= 2.4 \times 10^7$ s^{-1}: ——— $E_{act} = 6.0$ kcal/mol; - - - 7.0 kcal/mol; ••• 8.0 kcal/mol with $A = 10^{12}$ ($k_f^0 = 1.3 \times 10^8$ s^{-1} for **2** and 5.8×10^7 s^{-1} for **3**).

According to the original Orlandi−Siebrand theoretical treatment of stilbene isomerization, the small barrier for singlet-state torsion is the result of an avoided crossing between the lowest energy singlet excited ^{1}B state (^{1}S*) and a higher energy doubly excited ^{1}A state.[32] Subsequent theoretical treatments also

(30) The temperature dependence η for isopentane (1.35691−0.00055*(t − 15) where t is in °C) may be obtained from the following reference: Timmermans, J. *Physico-Chemical Constants of Pure Organic Compounds*; Elsevier: New York, 1950; Vol. 1.

(31) For a discussion of nonintegral refractive index exponents see: Shibuya, T. *Chem. Phys. Lett.* **1983**, *103*, 46 and reference 22.

Scheme 1

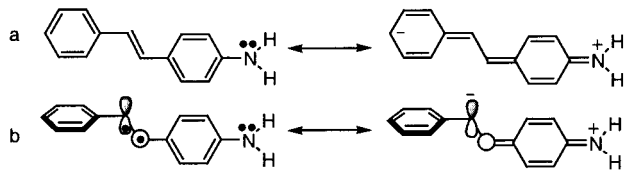

indicate the presence of a small thermal barrier on the singlet-state surface.[33] The experimental evidence as summarized by Saltiel indicates that the barrier height is approximately 3.5 kcal/mol and that the planar ^{1}S* and perpendicular ^{1}P* states are approximately isoenergetic.[34] Internal conversion from ^{1}P* to the ground state is sufficiently rapid ($k_{ic} \geq 10^{12}$ s^{-1}) to render conversion of ^{1}S* → ^{1}P* largely irreversible, despite the low barrier for the reverse process.[34]

To a first approximation, the height of the barrier for singlet-state torsion should be dependent upon the relative energies of the planar ^{1}S* and perpendicular ^{1}P* states, lowering the energy of ^{1}P* relative to ^{1}S* decreasing the barrier and increasing the energy of ^{1}P* relative to ^{1}S* increasing the barrier.[35] The relative energies of ^{1}S* can be estimated from the positions of their 0,0 transitions (Table 1). The 0,0 energies of **3** and **4** are approximately 7 kcal/mol lower than that of **1**[36] and the energy of **2** is an additional 4 kcal/mol lower (Table 1). Extended or through-conjugation is presumably responsible for the stabilization of **4** (Scheme 1a). Extended conjugation is not possible for **3** and is of reduced importance for **2** due to the large styryl−aniline dihedral angle. The 0,0 energies of both **2** and **3** are lowered by splitting of the lowest transition due to configuration interaction (Figure 1 and Table 1) which is largely responsible for the lower singlet energies of **2** and **3**.

The nature of the twisted ^{1}P* state is the subject of continuing controversy. Michl and Bonačić-Koutecký have described ^{1}P* for simple alkenes as a resonance hybrid of biradical and charge-transfer configurations (eq 5).[37,38]

$$\psi_{P^*} = c_1\psi_{\text{biradical}(A^{\bullet}B^{\bullet})} + c_2\psi_{CT(A^+B^-)} + c_3\psi_{CT(A^-B^+)} \quad (5)$$

An electron-donating or electron-withdrawing para-substituent would be expected to stabilize one of the two charge-transfer configurations and thus lower the energy of ^{1}P*. Evidently, the *para*-amino substituent in **4** stabilizes ^{1}P* (Scheme 1b) to approximately the same extent that it stabilizes ^{1}S* (∼7 kcal/mol). This would result in a barrier for singlet state torsion similar to that of **1** (Figure 6), in accord with experimental observation.

In the case of **3**, the *meta*-amino substituent cannot stabilize the charge-transfer configuration of ^{1}P* by resonance. Dewar et al.[39] have calculated that the heats of formation of the 4- and 3-aminobenzyl cations using the MINDO Hamiltonian and find the 3-aminobenzyl cation to be 24 kcal/mol less stable! This difference is also reflected in the Hammett σ^+_{para} and σ_{meta} parameters for the amino group (−1.3 and −0.16, respectively).[40] The difference in these values is the largest for any substituent in a standard tabulation of Hammett parameters.[40] In the absence of a stabilized charge-transfer configuration (eq 5), the energy of ^{1}P* for **3** should be similar to that of **1**. Since the energy of ^{1}S* in **3** is ∼7 kcal/mol more stable than for **1** this should result in endergonic torsion with a barrier ≥7 kcal/mol (Figure 6), in accord with experimental observation.

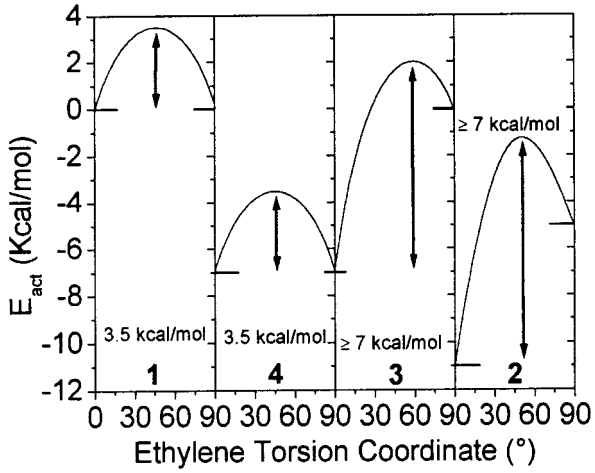

Figure 6. Potential energy diagram for ethylene bond torsion in the lowest excited state for **1**−**4** in nonpolar solvents. Energies relative to ^{1}S* for stilbene.

In the case of **2** resonance stabilization of ^{1}P* is expected to be smaller than that for **4** due to nonbonded repulsion between the amine and styryl substituents. AM1 minimization of the twisted geometry expected for ^{1}P* provides a dihedral angle of 31° between the amine and benzyl groups, somewhat smaller than the value for S_0 (45−48°). Nakata et al.[41] have computed the destabilization energy of benzylic cations upon rotation of the phenyl−methylene bond at the RHF/6−31 G* level and find that it obeys a $\cos^2(\theta)$ dependence. Thus, the resonance stabilization energy of ^{1}P* in **2** might be expected to be approximately 3/4 as large as that in **4** (∼5 kcal/mol). However, since the stabilization of ^{1}S* is 11 kcal/mol, twisting should be endergonic with a barrier >6 kcal mol (Figure 6), in accord with experimental observations.

Concluding Remarks. In summary, the exceptionally long singlet lifetimes for the *ortho*- and *meta*-aminostilbenes **2** and **3** are a consequence of large barriers for torsion (>7 kcal/mol) on the singlet state surface and small fluorescence rate constants. Therefore, **2** and **3** decay exclusively via fluorescence and intersystem crossing to the triplet, which undergoes barrierless torsion about the ethylene bond.[1,42] In nonpolar solvents, fluorescence is the major decay pathway, and thus the singlet lifetime is determined mainly by the fluorescence rate constant which is larger for **2** than for **3**. Increasing the solvent polarity results in a decrease in the fluorescence rate constant and an increase in singlet lifetime. The calculated rate constants for intersystem crossing for **2** and **3** (∼2×10^7 s^{-1}) are similar to the estimated value for *trans*-stilbene.[1]

The large barriers for singlet state torsion in **2** and **3** both result from greater stabilization of ^{1}S* vs ^{1}P*. However, the

(32) (a) Orlandi, G.; Siebrand, W. *Chem. Phys. Lett.* **1975**, *30*, 352. (b) Orlandi, G.; Palmieri, P.; Poggi, G. *J. Am. Chem. Soc.* **1979**, *101*, 3492.
(33) (a) Hohlneicher, G.; Dick, B. *J. Photochem.* **1984**, *27*, 215. (b) Troe, J.; Weitzel, K.-M. *J. Chem. Phys.* **1988**, *88*, 7030.
(34) Saltiel, J.; Waller, A. S.; Sears, D. F., Jr. *J. Am. Chem. Soc.* **1993**, *115*, 2453.
(35) (a) Hammond, G. S.; *J. Am. Chem. Soc.* **1955**, *77*, 334. (b) Leffler, J. E.; Grunwald, E. *Rates and Equilibria of Organic Reactions*; Wiley: New York, 1963.
(36) Dyck, R. H.; McClure, D. S. *J. Chem. Phys.* **1962**, *36*, 2326.
(37) Bonačić-Koutecký, V.; Köhler, J.; Michl J. *Chem. Phys. Lett.* **1984**, *104*, 440.
(38) Bonačić-Koutecký, V.; Michl J. *J. Am. Chem. Soc.* **1985**, *107*, 1765.
(39) Dewar, M. J. S.; Landman, D. *J. Am. Chem. Soc.* **1977**, *99*, 7439.
(40) Brown, H. C.; Okamoto, Y. *J. Am. Chem. Soc.* **1958**, *80*, 4979.
(41) Nakata, K.; Fujio, M.; Saeki, Y.; Mishima, M.; Tsuno, Y.; Nishimoto, K. *J. Phys. Org. Chem.* **1996**, *9*, 573.
(42) (a) Saltiel, J.; Chang, D. W. L.; Megarity, E. D.; Rousseau, A. D.; Shannon, P. T.; Thomas, B.; Uriarte, A. K. *Pure Appl. Chem.* **1975**, *41*, 559. (b) Ni, T.; Caldwell, R. A.; Melton, L. A. *J. Am. Chem. Soc.* **1989**, *111*, 457.

origin of these barriers is somewhat different for the two isomers. In both cases ^{1}S* is stabilized by splitting of the lowest singlet state resulting from configuration interaction, the stabilization being larger for **2** than for **3**. In the case of **3** the *meta*-amino substituent is unable to stabilize the charge-transfer configuration of the twisted intermediate ^{1}P*. In the case of **2**, resonance stabilization of the charge-transfer configuration of ^{1}P* by the *ortho*-amino substituent is possible, but the magnitude of the stabilization is diminished by nonbonded interactions. Elucidation of the origin of the barrier for singlet-state torsion in **2** and **3** provides an explanation for the "meta effect" previously reported for several donor−acceptor disubstituted stilbenes.[5] We suggested that the long-lived fluorescent state for these stilbene derivatives might have TICT (twisted intramolecular charge-transfer) character with twisting about the aniline−styrene single bond. The current results suggest that there is no need to invoke TICT character for the fluorescent ^{1}S* states of the aminostilbenes.

The amino substituent is apparently unique in its ability to dramatically increase the barrier for singlet-state isomerization of a meta- or ortho-monosubstituted stilbene. A search of the literature reveals that this effect was nearly discovered 30 years ago by Güsten and co-workers.[6] They reported the photoisomerization quantum yields for seven para- and seven meta-substituted stilbenes in cyclohexane, all of which had quantum yields for trans → cis isomerization >0.3. The amino group was included among the para-substituents but not the meta compounds. They subsequently reported the quantum yields for photocyclization of the cis isomers of both **3** and **4**.[10] The quantum yields reported for photoisomerization of the *para*- and *meta*-methoxystilbenes are 0.40 and 0.31, suggesting that the barrier for photoisomerization of the meta isomer is not unusually large.[6] Investigations of ortho-substituted stilbenes appear to be limited to methyl substituents. The small fluorescence quantum yield reported for 2,4,6-trimethylstilbene (ϕ_f = 0.003) suggests that it has a small barrier for singlet torsion.[9] The ortho-methyl substituents might be expected to stabilize ^{1}P* more than ^{1}S*.

The photochemistry of 4,4′-disubstitued stilbenes has recently been the subject of extensive investigations. A high barrier for photoisomerization of singlet 4,4′-dimethoxystilbene[23,43] and high fluorescence quantum yields for 4,4′-diaminostilbenes[24] and for several donor−acceptor stilbenes, including 3′-amino-4-methoxycarbonylstilbene[5] have been reported. In these examples it seems likely that the substituents lower the energy of fluorescent ^{1}S* state more than that of the ^{1}P* state. Papper et al.[44] have studied a variety of donor and acceptor stilbene and find low barriers for singlet isomerization with relatively weak donors (methoxy, methyl, and halogen) but large barriers for the stronger dimethylamino donor. They have correlated their results with the difference in the Hammett constants for the two substituents.[44]

Lapouyade et al.[7] compared the photophysical behavior of *meta*- vs *para*-nitro-4′-dimethylaminostilbene and found the meta isomer to have a significantly lower ϕ_f than the para isomer. Simple resonance arguments suggest that moving an electron-withdrawing substituent from the para to the meta position should stabilize ^{1}P* (eq 5) more than ^{1}S* and hence lower the torsional barrier. Thus, the amino group, when present at the meta or ortho position, may be unique in its ability to prolong the singlet lifetime of donor−acceptor-substituted stilbenes as well as monosubstituted stilbenes.

The greatly diminished reactivity of **3** vs **4** toward singlet state photoisomerization follows the normal ground state pattern for meta vs para electron-donating substituents. This result stands in contrast to the enhanced reactivity of meta- vs para-substituted methoxylated benzyl acetates toward photochemical solvolysis, an example of the so-called "meta effect" (or "meta−ortho effect") which has been investigated extensively by Zimmerman and others.[8] Clearly electronic transmission in the excited state determines the effects of substituents on stilbene photoisomerization as well as benzyl acetate solvolysis. However the consequences are not the same.

Whereas an amino group in the ortho or meta position may be unique in its ability to increase the stilbene singlet lifetime, it may be possible to generalize the model presented in Figure 6 to other unimolecular photochemical reactions. Whenever an activated nonradiative decay pathway competes with nonactivated fluorescence and intersystem crossing, it should be possible to alter the singlet lifetime by changing the barrier for the activated process. Substituents which stabilize the fluorescent singlet state more than the transition state for the activated pathway will increase barrier and hence the singlet lifetime, whereas substituents which stabilize the transition state more than the singlet state will lower the barrier and decrease the singlet lifetime. In cases where the activated process leads to product formation, the efficiency of product formation will also be affected.

Experimental Section

Materials. The *trans*-aminostilbenes **2**−**4** were prepared by the standard Wittig route.[45] Corresponding *ortho*-, *meta*-, *para*-nitrobenzaldehydes (Aldrich) were reacted with triphenylphosphonium chloride (Aldrich) in a CH_2Cl_2−H_2O dual phase system using tetrabutylammonium iodide (Aldrich) as a phase-transfer catalyst (10 mol %). The reaction mixture was stirred at room temperature overnight under a N_2 atmosphere. After the reaction was complete, the CH_2Cl_2 layer was separated and washed with brine several times. Purification was carried out by column chromatography (SiO_2/hexanes−EtOAc (80:20), 230−400 mesh SiO_2) to remove the cis isomer. If necessary, the trans isomer was enriched by refluxing a cis−trans mixture in benzene using a catalytic amount of I_2 prior to chromatography. The trans isomers were further purified by recrystallization from MeOH to yield a pale yellow solid (**2**: mp = 105−106 °C, lit. mp[46] = 102−105 °C; **3**: mp = 119−120 °C, lit. mp[47] = 120−121 °C; **4**: mp = 153−154 °C, lit. mp[10] = 151 °C). Typical overall yields of the trans isomer were 40%. Reduction of the nitro group to the amino group was carried out using Zn/HCl−AcOH as the reducing agent.[48] Typical yields from the reduction were 85%. Purification of the corresponding *trans*-aminostilbene was carried out by recrystallization from HPLC grade MeOH. All materials were found to have greater than 98.5% trans isomer as estimated by GLC. ^{1}H NMR and HRMS was done to establish that the identity of all compounds. All solvents used for spectroscopy were either spectrophotometric or HPLC grade (Fisher) and were used as received. Hexanes was used instead of hexane as a solvent for all spectroscopic measurements.

Methods. ^{1}H NMR spectra were measured on a Varian Gemini 300 spectrometer. GLC analysis was performed using a Hewlett-Packard HP 5890 instrument equipped with a HP1 poly(dimethylsiloxane) capillary column. UV−vis spectra were measured on a Hewlett-Packard 8452A diode array spectrometer using a 1 cm path length quartz cell. Fluorescence spectra were measured on a SPEX Fluoromax spectrometer. Low-temperature spectra were measured either in a Suprasil quartz

(43) Saltiel, J.; Waller, A. S.; Sears, D. F.; Hoburg, E. A.; Zeglinski, D. M.; Waldeck, D. H. *J. Phys. Chem.* **1994**, *98*, 10689.
(44) Papper, V.; Pines, D.; Likhtenshtein, G.; Pines, E. *J. Photochem. Photobiol., A* **1997**, *111*, 87.
(45) Lee, B. H.; Marvel, C. S. *J. Polym. Sci. Chem. Ed.* **1982**, *20*, 393.
(46) Ziegler, C. B.; Heck, R. F. *J. Org. Chem.* **1978**, *43*, 2941.
(47) Boyer, J. H.; Alul, H. *J. Am. Chem. Soc.* **1959**, *81*, 2136.
(48) Taylor, T. W. J.; Hobson, P. M. *J. Chem. Soc.* **1936**, 181.

EPR tube using a quartz liquid nitrogen coldfinger dewar at 77K or in a Oxford Cryogenics DN1704 cryostat fitted with a Oxford Instruments ITC4 temperature controller. Anthracene (**2** and **4**, $\Phi_f = 0.27$[49]) or phenanthrene (**3**, $\Phi_f = 0.14$[50]) was used as a external standard for the measurement of fluorescence quantum yields. Fluorescence quantum yields were measured by comparing the integrated area under the fluorescence curve for the *trans*-aminostilbenes and the standard at equal absorbance at the same excitation wavelength. All fluorescence spectra are uncorrected, and the estimated error for the fluorescence quantum yields is ±10%, although the quantum yields were corrected for the refractive index of the solvent. Fluorescence decays were measured either on a Photon Technologies International LS-1 single photon counting apparatus with a gated hydrogen arc lamp using a scatter solution to profile the lamp or on a Photon Technologies International Timemaster stroboscopic detection instrument with a gated hydrogen or nitrogen lamp using a scatter solution to profile the instrument response function. Nonlinear least-squares fitting of the decay curves were fitted using the Levenburg−Marquardt algorithm as described by James et al.[51] as implemented by the Photon Technologies International Timemaster (version 1.2) software. Goodness of fit was determined by judging the χ^2 (<1.3 in all cases), the residuals, and the Durbin−Watson parameter (>1.6 in all cases). Measurements of quantum yields of photoisomerization for **2** and **3** were measured on optically dense degassed solutions ($\sim 10^{-3}$ M) using an excitation wavelength of 313 nm, and the extent of photoisomerization (<5%) was quantified using GLC. Quantum yields of photoisomerization for **4** (<10% conversion) were determined by changes in absorbance at 2 wavelengths before and after irradiation at 313 nm. For this purpose, the cis isomer of **4** was synthesized using the above methodology and its molar absorptivity determined. Excitation at 313 nm was achieved using a 150 W medium-pressure mercury arc lamp filtered through an alkaline potassium dichromate solution (**2** and **3**) or a 150 W xenon lamp filtered through a Bausch and Lomb high-intensity monochromator (**4**). All spectroscopic measurements were performed on solutions that were purged with dry N_2 for 20−25 min. In some cases, solutions were degassed under vacuum (<10^{-4} Torr) through five freeze−pump−thaw cycles and flame-sealed to establish the validity of the N_2-purged experiments. INDO/S-CIS-SCF (ZINDO) calculations (nine occupied and nine unoccupied frontier orbitals) were performed on a Macintosh IIfx computer using the ZINDO Hamiltonian as implemented by Cache Release 3.5.[29,52] All structures used in the ZINDO calculations were based on ground state, SCF/AM1, optimized geometries using the MOPAC (version 94.10) suite of programs as implemented under Cache Release 3.5.[52] Gaussian fitting procedures were carried out using GRAMS/386 (version 3) software on a IBM-compatible PC running Windows 3.1.[53]

Acknowledgment. We are grateful to Professors Jack Saltiel and Siegfried Schneider for helpful discussions. Funding for this project was provided by NSF grant CHE-9734941.

Supporting Information Available: ZINDO optimized frontier orbitals for **2** and **4**, kinetic modeling of the low-temperature singlet lifetime data for **2** and **3** in isopentane, and ZINDO calculated energies for the rotamers of **2** and **3** (PDF). This material is available free of charge via the Internet at http://pubs.acs.org.

JA992335Q

(49) Dawson, W. R.; Windsor, M. W. *J. Phys. Chem.* **1968**, *72*, 3251.
(50) Birks, J. B. *Photophysics of Aromatic Molecules*; John Wiley And Sons: New York, 1970.
(51) James, D. R.; Siemiarczuk, A.; Ware, W. R. *Rev. Sci. Instrum.* **1992**, *63*, 1710.
(52) Oxford Molecular Group, Inc., Campbell, CA 95008. Telephone: (800) 876−9994. Web site: http://www.oxmol.com.
(53) Galactic Industries Corp., Salem, NH 03079. Telephone: (603) 898 7600. Web site: http://www.galactic.com/.